EXEMPLARY DETERMINATION OF THE ADHESION ELLIPSES BASED ON SIMULATION OF AN ACCELERATING MOTOR VEHICLE

Jarosław Zalewski

Warsaw University of Technology, Warsaw, Poland

E-mail of corresponding author: jaroslaw.zalewski@pw.edu.pl

Jarosław Zalewski 0000-0002-7559-0119

Resume

In the paper, some selected results concerning the ellipses of adhesion for various conditions of motion of a vehicle model, have been presented. The analysis, regarding the phenomena between the road and the wheels of the given motor vehicle's model, was previously carried out in the earlier paper by the author. However, they proved useful for the second part of research based on determination of the ellipses of adhesion. This can enable answering the question whether the road conditions may affect the maximum longitudinal and lateral forces combining such ellipses in the contact plane between the road and the wheels. The analysis has been presented based on the previously obtained results.

Article info

Received 22 March 2024
Accepted 15 May 2024
Online 28 May 2024

Keywords:

ellipses of adhesion
contact forces between a wheel and a road

Available online: https://doi.org/10.26552/com.C.2024.032

ISSN 1335-4205 (print version)
ISSN 2585-7878 (online version)

1 Introduction

The ability of a motor vehicle to develop a full adhesion between its wheels and the road is one of the most crucial feature, among others in terms of the road traffic safety. One of the maneuvers requiring the adhesion is accelerating when, depending on the road conditions, it may not be fully developed and the wheels may either slip or partially lose contact with the road, especially with the random irregularities occurring. Multiple researches on the adhesion between the wheels and the road have so far been conducted, both form the point of view of the rubber ingredients, e.g. in [1-2] and the road conditions, e.g. in [3-5].

However, research on the adhesion does not consider only the above mentioned aspects. Determining the characteristics useful for further research also plays an important role which has been presented, e.g. in [6-8]. Moreover, determination of the adhesion coefficient in various conditions of motion of road vehicles can give answers, e.g., which road conditions tend to be the least beneficial for safe driving. This has been undertaken, among others in [9-12] up to the wheel blocking conditions [13] and analysis of the discussed phenomena for the electric vehicles [14]. One of the considered problems was the influence of the icy road on the friction between the tire and a surface.

Of course, it seems important to be acquainted with the problems of road irregularities, especially when the randomness is taken into account. Some works, including, e.g., [15-17], have been devoted to these problems. Some papers have been devoted to more specific aspects, such as determining the road conditions via a signal obtained from the vehicle [18], using measurements for vehicle dynamics simulations [19], or nonlinearity included in the problem of the wheel - road contact phenomena on a randomly uneven road [20].

The aim of this paper was to present the possibility of determining the ellipses of adhesion between the wheels and the road with the use of results obtained for a specific maneuver of vehicle's acceleration simulated in MSC/Adams environment. The selected results of the simulations have previously been presented in [21] by the author and were used as a basis to determine the ellipses of adhesion between the wheels and the road for various adopted conditions of motion. The paper [21] is a source for the research presented here and the main question is whether the longitudinal and the lateral forces, occurring between the wheels and the road, can combine to produce such ellipses and whether the

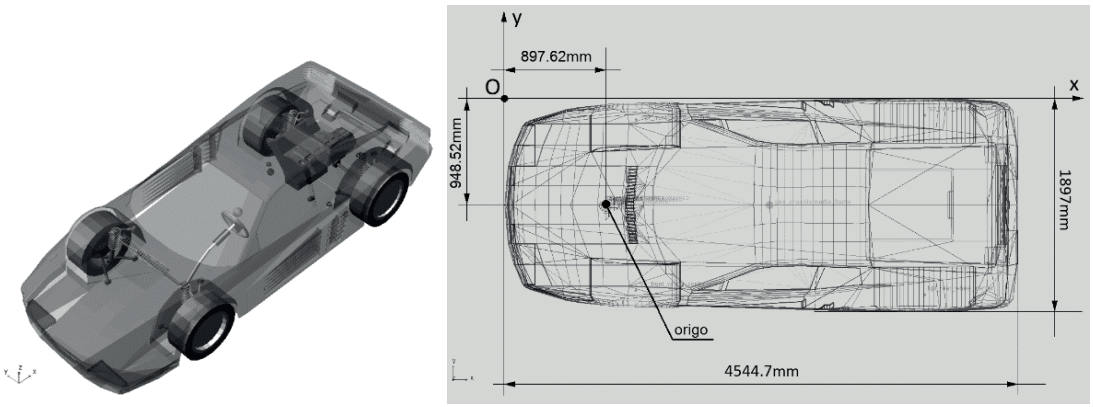

Figure 1 *The vehicle's model used in simulations and the location of the "origo" point [based on MSC Adams/Car]*

Table 1 *Mass - inertia parameters of the unladen simulated vehicle model [21]*

	Unladen vehicle	Laden vehicle
Mass	1528kg	1686kg
Center of mass location relative to the "origo"	x_c = 1.75m, y_c = -0.0014m, z_c = 0.43m	x_c = 1.73m, y_c = -0.007m, z_c = 0.435m
Moment of inertia (I_x) relative to the X axis	583kg·m^2	618kg·m^2
Moment of inertia (I_y) relative to the Y axis	6129kg·m^2	6550kg·m^2
Moment of inertia (I_z) relative to the Z axis	6022kg·m^2	6409kg·m^2
Moment of deviation (I_{xy}) versus the XY axes	-1.9kg·m^2	1.95kg·m^2
Moment of deviation (I_{xz}) versus the XZ axes	1160kg·m^2	1276kg·m^2
Moment of deviation (I_{yz}) versus the YZ axes	-1.3kg·m^2	0.51kg·m^2

random irregularities and the icy road surface have any influence on these ellipses.

The significance of research presented below is focused on understanding if the lateral and the longitudinal forces in the area of a mutual contact between the road and the wheels can compose an ellipse of adhesion and if such an ellipse can be a factor determining the nature of the wheel - road cooperation, as well as to what degree it could be a feature specifying the road traffic safety.

2 Assumptions for the adopted maneuver

In order to present the discussed problem in a proper way it is fair to recall the basic assumptions made in [21] so that determination of the adhesion ellipses would be presented for the specific conditions of motion and the specific maneuver.

A double seater model was used (Figure 1) in the simulations performed in Adams/Car. This model has previously been used in several works by the author for various maneuvers. Although the general assumptions remained the same, e.g., as in [21] the whole mass of a vehicle was changed by adding different masses representing a driver, a passenger, and a baggage. In [21] they were altered as in Table 1. The new coordinates of the center of mass and the moments of inertia and deviation after loading were calculated by Adams/Car in relation to the so-called "origo" point (Figure 1), which is a point moving along with the vehicle but located on the road.

The vehicle's double seater model used in [21] had the FTIRE (flexible) tires because they allowed running the simulations on the randomly uneven road. This means that a single irregularity can be shorter than the length of the contact area between the wheel and a road. The springs in the MacPherson columns in the vehicle's suspension was linear and the dampers were non-linear. The vehicle's body was assumed rigid to provide the analysis of a multibody without any deformations or micro deformations within its structure.

The simulations in [21] were run for various road conditions with the initial speed 20 km·h^{-1} and the road conditions adopted as configurations presented in Table 2, mainly regarding the road surface (dry or icy) and the maximum amplitudes of the random irregularities, which were specified by the intensity parameter. Moreover, the difference between the road profiles for the left and the right wheels was specified by the cor_{rl} parameter, which, in this case, provided almost different profiles for both sides of the vehicle enabling greater reality. The most difficult conditions of motion were adopted for the configurations 7 and 8 as in Table 2, which was more exactly discussed in [21].

The road was randomly uneven in each configuration,

Table 2 *The configurations of the road conditions adopted for the simulations [21]*

	Road	Road condition	Intensity	Corrl	Initial V [km · h^{-1}]
Configuration 1	flat	dry	-	-	20
Configuration 2	flat	icy	-	-	20
Configuration 3	uneven	dry	0.5	0.2	20
Configuration 4	uneven	icy	0.5	0.2	20
Configuration 5	uneven	dry	1.0	0.2	20
Configuration 6	uneven	icy	1.0	0.2	20
Configuration 7	uneven	dry	1.5	0.2	20
Configuration 8	uneven	icy	1.5	0.2	20

except for 1 and 2. Moreover, the icy road means that the coefficient of adhesion between the wheels and the road was set to 0.3 and the dry road had its value set at 0.8. In all the configurations it was the same for each wheel. The assumed values reflect the average coefficient on a dry and an icy road.

Although the acceleration maneuver was performed for the initial speed of 20 km·h^{-1}, the vehicle started accelerating after the first 2s of the simulation (which lasted for 10 s) as if it was moving with the initial speed for the first 2s. After the next 0.5 s the vehicle had the full throttle on, and it meant only a short period to start fully accelerating.

The intensity parameter used specifically in MSC/Adams Car is a coefficient determining the amplitudes of the road irregularities in the random profiles. To mark the differences caused in the profiles by intensity, three exemplary road profiles were presented in [21] and repeated here in Figures 2, 3 and 4 for three values of intensity, 0.5, 1 and 1.5, respectively. Although it is not clearly specified how the intensity is related to the road profile in MSC/Adams Car, in several tutorials it has been marked that these profiles are prepared in accordance with the ISO standards. One of the aims of this paper was to examine whether the greater intensity would alter the ellipses of adhesion and that is why it was increased even to 1.5, given that [21] is a background for the analyses presented here.

As for the random irregularities in a stochastic uneven road, their generation has been described in many MSC/Adams tutorials (e.g. [22]). These irregularities are easily dealt with by Adams/Car thanks to the FTIRE

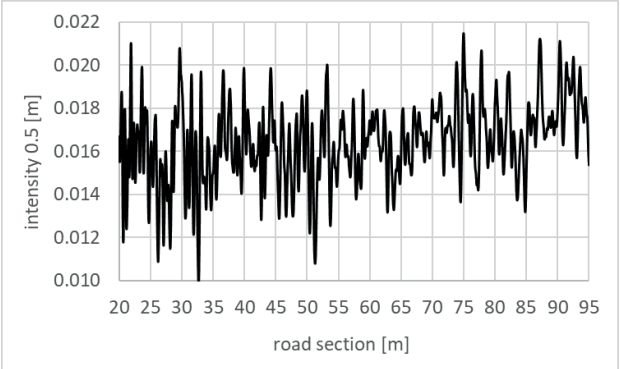

Figure 2 *Road profile for the selected road section between 20th and 95th meter at the intensity = 0.5 [21], based on Adams/Car*

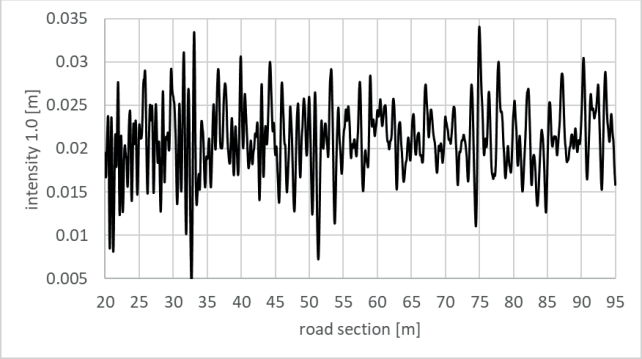

Figure 3 *Road profile for the selected road section between 20th and 95th meter at the intensity = 1 [21], based on Adams/Car*

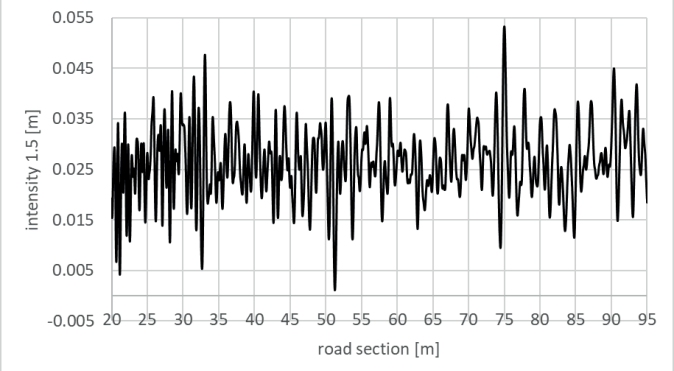

Figure 4 *Road profile for the selected road section between 20th and 95th meter at the intensity = 1.5 [21], based on Adams/Car*

(flexible tire) model, also described in, e.g. [22], which allows recognition of the holes and bumps in the road, which are up to twice shorter than the length of the area of the mutual contact between the wheels and the road (let us call it the contact patch as, e.g. in [22]). For the purpose of this paper it was assumed that the holes shorter than half of this contact patch can be omitted in the analysis, but the bumps can influence the vehicle's behavior.

More on the intensity and its relation to the maximum amplitudes of the irregularities of the road profiles used for the purposes of this paper, one can read, e.g., in [21].

In [21] it was also stressed that the discussed example of the acceleration maneuver was performed for the steering wheel locked to maintain the straightforward direction, which seems obvious when driving on a straight part of a road. However, another possibility taken into account for further research may involve free (no handling) motion with the acting disturbances causing the vehicle to deviate from the assumed straightforward direction.

3 Analysis of results related to the road - wheel adhesion

During each simulation one of the components calculated by Adams/Car were the contact forces between the wheels and the road. The measurement was conducted with the use of the virtual sensors, which are located at various points in the vehicle's model. Hence, the maximum absolute values of these contact forces were determined based on the internal measuring system of Adams.

To draw some necessary conclusions, some simple formulas should be introduced at first. The ellipse of adhesion should be based on the maximum values of the coefficient of adhesion in two directions: longitudinal and lateral in relation to the direction of motion of the vehicle's model. Therefore, the first formula used here allows determination of these coefficients. This formula is ok, typical for each book on motor vehicle dynamics.

$$\mu_{ix} = \frac{F_{ix}}{G_i},\ \mu_{iy} = \frac{F_{iy}}{G_i}, \tag{1}$$

where:

μ_{ix} - the coefficient of adhesion in the longitudinal direction (along the direction of motion of a vehicle) for the i-th wheel,

μ_{iy} - the coefficient of adhesion in the lateral direction (perpendicular to the direction of motion of a vehicle) for the i-th wheel,

F_{ix} - the maximum absolute contact force in the longitudinal direction (along the direction of motion of a vehicle) for the i-th wheel,

F_{iy} - the maximum absolute contact force in the lateral direction (perpendicular the direction of motion of a vehicle) for the i-th wheel,

G_i - the force loading the i-th wheel and normal to the contact plane between this wheel and the road.

The second formula was used to specify the equation of each ellipse of adhesion to use the obtained coefficient to calculate this ellipse, e.g., in Excel. It is also simply used to build an ellipse based on the maximum values of its axes only. It is worth noticing that the paper presents the ellipses of adhesion as a maximum available areas of a contact between the wheels and the road for various conditions of motion.

$$x_i = \mu_{ix}\cos\alpha,\ y_i = \mu_{iy}\sin\alpha, \tag{2}$$

where:

μ_{ix} - the coefficient of adhesion in the longitudinal direction (along the direction of motion of a vehicle) for the i-th wheel,

μ_{iy} - the coefficient of adhesion in the lateral direction (perpendicular to the direction of motion of a vehicle) for the i-th wheel,

x_i - the values along the longitudinal axis of the ellipse of adhesion for the i-th wheel,

y_i - the values along the lateral axis of the ellipse of adhesion for the i-th wheel,

α - the angle used in specifying the ellipses of adhesion, ranging from 0° to 360°.

The first set of results was related to braking on a flat and dry road (configuration 1). In Table 3 the

Table 3 *The forces between the road and the wheels for configuration 1 [21]*

	Left front wheel (LF)			Right front wheel (RF)		
	F_{Xmax} [N]	F_{Ymax} [N]	F_{Zmax} [N]	F_{Xmax} [N]	F_{Ymax} [N]	F_{Zmax} [N]
Max absolute	166.08	604.31	3874.66	167.57	634.3	3946.36
	Left rear wheel (LR)			Right rear wheel (RR)		
	F_{Xmax} [N]	F_{Ymax} [N]	F_{Zmax} [N]	F_{Xmax} [N]	F_{Ymax} [N]	F_{Zmax} [N]
Max absolute	5289.13	2010.29	5564.94	5400.4	2003.81	5653.86

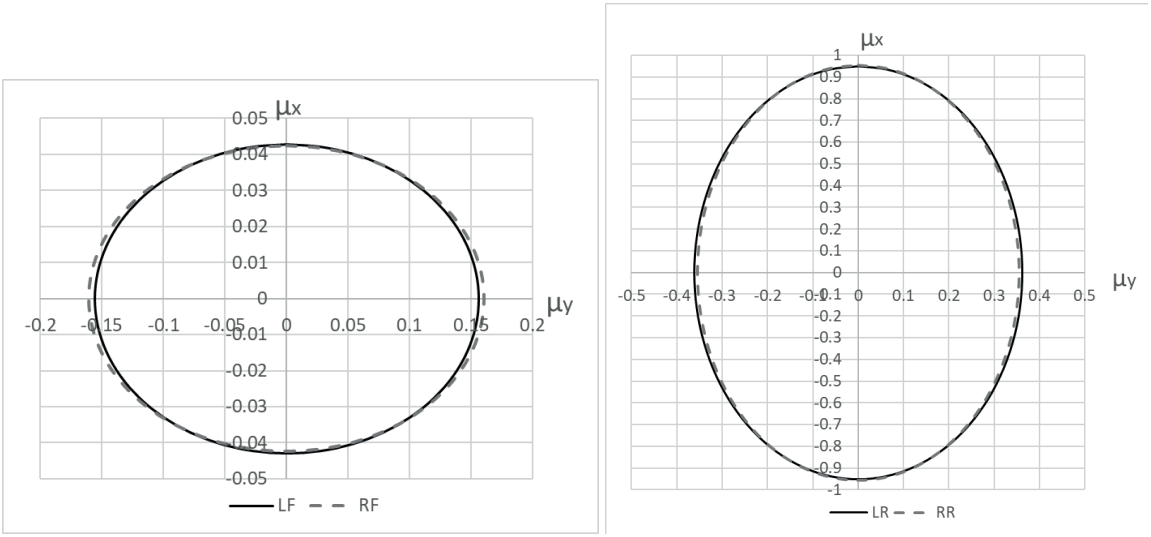

Figure 5 *Ellipses of adhesion between the wheels and the road for configuration 1*

Table 4 *The forces between the road and the wheels for configuration 2 [21]*

	Left front wheel (LF)			Right front wheel (RF)		
	F_{Xmax} [N]	F_{Ymax} [N]	F_{Zmax} [N]	F_{Xmax} [N]	F_{Ymax} [N]	F_{Zmax} [N]
Max absolute	317.05	481.68	3734.42	325.09	488.95	3827.46
	Left rear wheel (LR)			Right rear wheel (RR)		
	F_{Xmax} [N]	F_{Ymax} [N]	F_{Zmax} [N]	F_{Xmax} [N]	F_{Ymax} [N]	F_{Zmax} [N]
Max absolute	3357.03	1060.93	5783.71	3434.92	1148.62	5856.73

maximum absolute values of the forces acting on each wheel are presented based on the results obtained in [21], whereas in Figure 5 is shown the ellipse of adhesion based on the determined coefficients in Equation (1) and the Equation (2).

The markings in Table 1 denote the selected wheels for which the ellipses were determined, i.e., LF - left front, RF - right front, LR - left rear and RR - right rear. These markings were also used in Figure 5. The rest of the presented results have been marked in the same way.

It is important to stress that the calculated ellipses presented in this part of the paper, have been obtained for the maximum absolute values of the forces tangential and normal versus the plane of a mutual contact between the wheels and the road.

As it can be observed in Figure 5 the ellipse of adhesion has greater values of its axes for the rear wheels as the engine is located at the back of a vehicle. Despite braking, where usually the front wheels are extra loaded, the maximum coefficient μ_x here was only about 0.04 with about 0.95 for the rear wheels. The μ_y coefficient was also more than twice the magnitude for the rear (about 0.35) than for the front wheels (about 0.15).

The maximum absolute forces for configuration 2 are presented in Table 4, while in Figure 6 are shown the ellipses for this configuration. Here the ellipses for the front wheels show that the μ_x coefficient was twice greater than in the case of configuration 1, despite braking on the icy road. However, the μ_y coefficient was about 0.12, which is less than in the case of configuration 1. For the rear wheels the maximum μ_x coefficient was about 0.6, which is far less than in the case of configuration 1, whereas the μ_y coefficient was about 0.2, also less than for the dry road. It can be seen that braking on the icy road worsened the effectiveness for the rear wheels. Of course, both configurations (1 and 2) were adopted for a flat road surface.

The differences between the left and the right

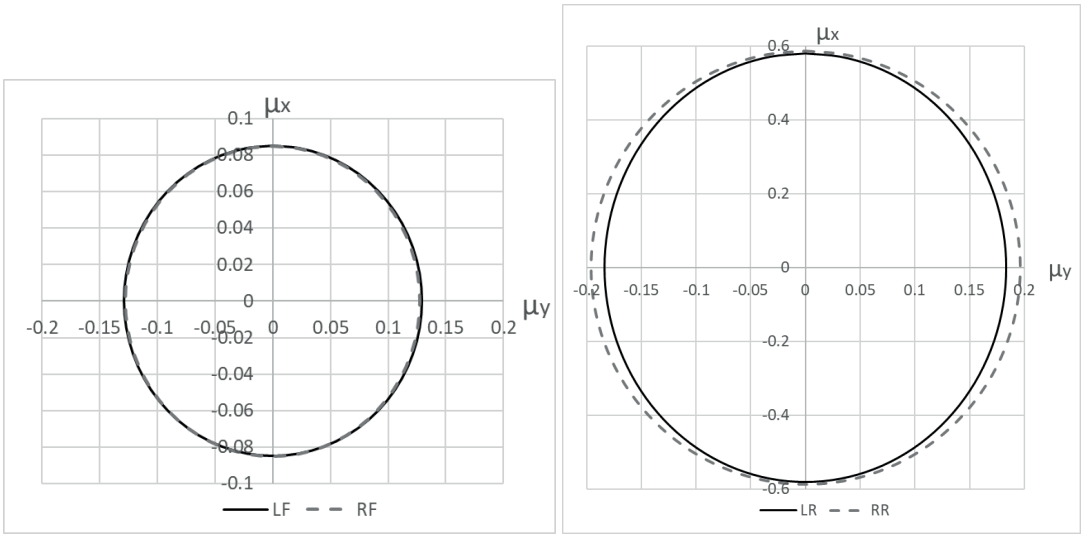

Figure 6 *Ellipses of adhesion between the wheels and the road for configuration 2*

Table 5 *The forces between the road and the wheels for configuration 3 [21]*

	Left front wheel (LF)			Right front wheel (RF)		
	F_{Xmax} [N]	F_{Ymax} [N]	F_{Zmax} [N]	F_{Xmax} [N]	F_{Ymax} [N]	F_{Zmax} [N]
Max absolute	995.51	723.65	4816.76	1051.4	452.45	5134.61
	Left rear wheel (LR)			Right rear wheel (RR)		
	F_{Xmax} [N]	F_{Ymax} [N]	F_{Zmax} [N]	F_{Xmax} [N]	F_{Ymax} [N]	F_{Zmax} [N]
Max absolute	7141.09	1296.05	7615.85	6474.63	1223.14	7636.4

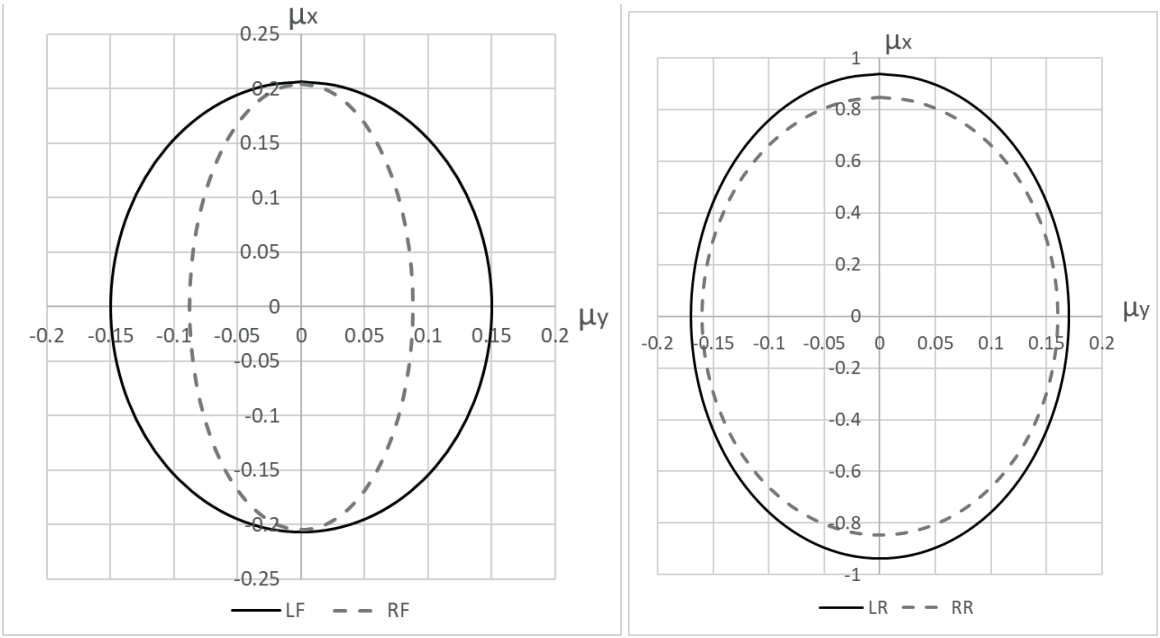

Figure 7 *Ellipses of adhesion between the wheels and the road for configuration 3*

wheels were marginal for the both configurations.

Let now analyze what effect the low amplitude irregularities (Figure 2, intensity 0.5) may cause in terms of the ellipses of adhesion. In Table 5 the results for the configuration 3 have been presented with the respective ellipses shown in Figure 7.

The ellipses for the front wheels show that the maximum μ_x coefficient was greater for both the left and the right wheels than in the case of configurations 1 and 2. However, the μ_y coefficient was different for the front wheels by about 0.05, which can be explained by the almost different road profiles adopted with the use of the cor_{rl} coefficient (Table 2). For the rear wheels the difference in the μ_x and μ_y coefficients was marginal and both wheels of the rear axis had almost the same maximum values (about 0.9 with little differences). This

Table 6 *The forces between the road and the wheels for configuration 4 [21]*

	Left front wheel (LF)			Right front wheel (RF)		
	F_{Xmax} [N]	F_{Ymax} [N]	F_{Zmax} [N]	F_{Xmax} [N]	F_{Ymax} [N]	F_{Zmax} [N]
Max absolute	867.39	565	5413.73	840.36	514.98	5653.29
	Left rear wheel (LR)			Right rear wheel (RR)		
	F_{Xmax} [N]	F_{Ymax} [N]	F_{Zmax} [N]	F_{Xmax} [N]	F_{Ymax} [N]	F_{Zmax} [N]
Max absolute	3156.29	1000.58	7009.33	3440.19	1157.3	7624

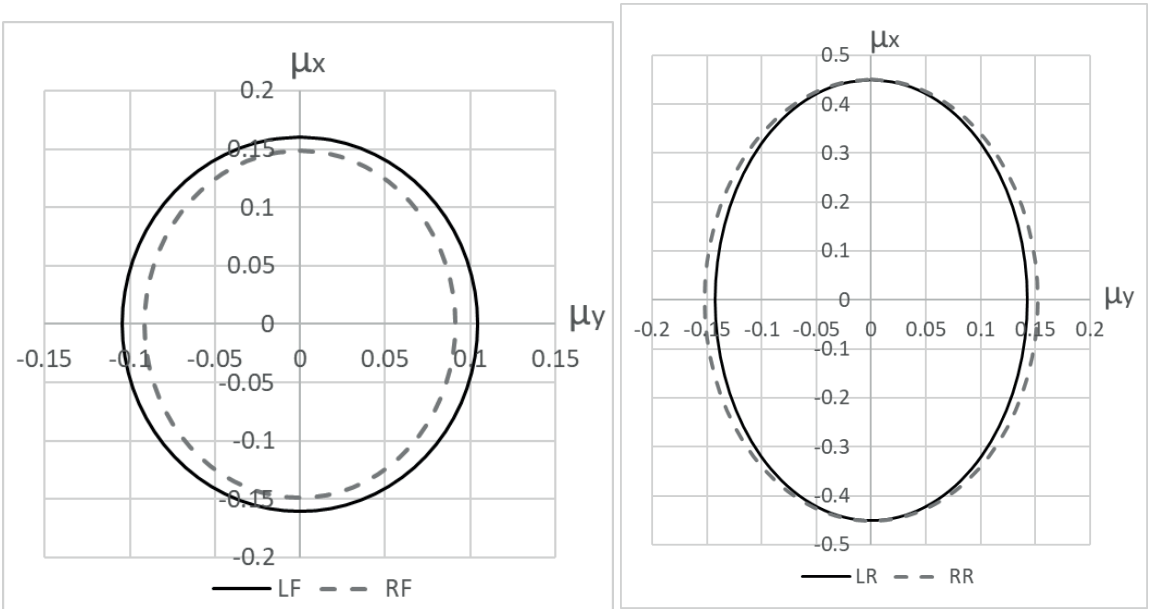

Figure 8 *Ellipses of adhesion between the wheels and the road for configuration 4*

Table 7 *The forces between the road and the wheels for configuration 5 [21]*

	Left front wheel (LF)			Right front wheel (RF)		
	F_{Xmax} [N]	F_{Ymax} [N]	F_{Zmax} [N]	F_{Xmax} [N]	F_{Ymax} [N]	F_{Zmax} [N]
Max absolute	1470	768	6700	1430.18	597.07	6868
	Left rear wheel (LR)			Right rear wheel (RR)		
	F_{Xmax} [N]	F_{Ymax} [N]	F_{Zmax} [N]	F_{Xmax} [N]	F_{Ymax} [N]	F_{Zmax} [N]
Max absolute	5761.58	1135.63	8935.27	7167.79	1146.32	9400

can be understood such that the engine acts as a mass loading the rear axle, which in these circumstances provided the understeering nature of a vehicle.

It is also necessary to mention that the motion during the braking, according to configuration 3, was performed on the dry road surface.

As for configuration 4 the additional factor was the icy road. The maximum values of the selected forces are presented in Table 6 and the ellipses of adhesion in Figure 8.

The μ_x coefficient for the front wheels was about 0.15 which is lower than in the case of configuration 3, with little differences between the left and the right wheels. The μ_y coefficient was about 0.1 and there were also some marginal differences between the left and the right wheel. It seems that in this case the icy road had also reduced the influence of the almost different road profiles.

As for the rear wheels, the maximum μ_x coefficient was about 0.45, which was twice less than for the dry road in configuration 3, and about 0.05 less than for the icy road in configuration 2. The μ_y coefficient was about 0.15 with almost no differences between the left and the right wheel, which means that the icy road, in combination with the low amplitude irregularities, had reduced the adhesion even more than in the case of configuration 2.

As for the motion on the more randomly uneven road, let move to the next results, i.e. configurations 5 and 6, where some additional observations can be made. In Table 7 the maximum forces between the wheels and the road have been shown, along with the ellipses of adhesion (Figure 9) obtained for them.

The μ_x coefficient for the front wheels was similar to that in configuration 3 on the dry road, i.e., about 0.2 with marginal differences between the left and the right

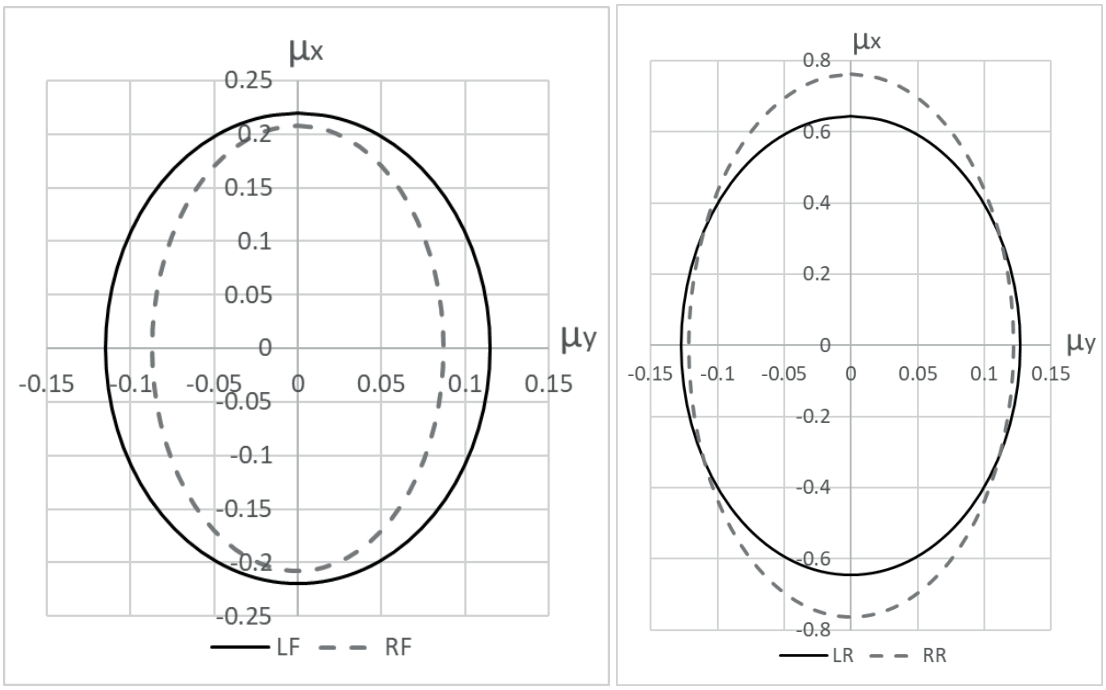

Figure 9 *Ellipses of adhesion between the wheels and the road for configuration 5*

Table 8 *The forces between the road and the wheels for configuration 6 [21]*

	Left front wheel (LF)			Right front wheel (RF)		
	F_{Xmax} [N]	F_{Ymax} [N]	F_{Zmax} [N]	F_{Xmax} [N]	F_{Ymax} [N]	F_{Zmax} [N]
Max absolute	1151.32	677.93	6703.52	1244	562.24	7218.32
	Left rear wheel (LR)			Right rear wheel (RR)		
	F_{Xmax} [N]	F_{Ymax} [N]	F_{Zmax} [N]	F_{Xmax} [N]	F_{Ymax} [N]	F_{Zmax} [N]
Max absolute	3012.9	1051.38	8560.18	2927.14	1036.44	8487.15

wheels. As for the differences in the μ_y coefficient, they were also marginal and amounted to about 0.12 for the left and 0.09 for the right wheel.

As for the rear wheels, the maximum μ_x coefficient was about 0.6 for the left and almost 0.8 for the right wheel, which seems strange when considering the motion on a dry, yet randomly uneven road. However, the almost different road profiles may have affected the vehicle's motion along with the slightly disturbed center of mass affected by loading the vehicle with a driver, a passenger and a baggage. The μ_y coefficient was almost the same for the left and the right wheel (about 0.12).

In Table 8 the maximum absolute forces for configuration 6 are presented, while the corresponding ellipses are presented in Figure 10. In this case the random irregularities of higher amplitudes (Figure 3) were covered with ice as an additional factor, which may have caused the disturbances of the vehicle's motion.

The ellipse for the front wheels shows that the μ_x coefficient was about 0.17, which was lower than for the dry road (configuration 5), and the μ_y coefficient 0.1 for the left and 0.08 for the right wheel. As for the rear wheels the μ_x coefficient was about 0.35, which was twice lower than in configuration 5, indicating the influence of both the icy road and the irregularities with higher amplitudes (intensity = 1.0). The maximum μ_x coefficient was about 0.12 for both rear wheels, similar as in configuration 5.

The last pair of results is presented in Tables 9 and 10, where the maximum absolute forces between the wheel and the road have been shown for configurations 7 and 8, respectively. The road conditions included the highest adopted amplitudes of the irregularities (Figure 4) in configuration 7 with the additional icy road in configuration 8.

The ellipses of adhesion for both configurations are presented in Figures 11 and 12 and discussed below.

The last set of results corresponds with the harshest of the adopted road conditions with the intensity of the road irregularities 1.5. Taking into account the almost different road profiles for the left and the right wheels, the μ_x coefficient in Figure 11was about 0.22 for the left front and 0.26 for the right front wheel, which is similar to the values obtained for configuration 5, also on a dry road. The μ_y coefficient was about 0.11, which is also similar to the results for configuration 5. For the rear wheels, however, the maximum μ_x coefficient was almost 0.8 for the left and almost 1 for the rear wheels, which is higher than in the case of configuration 5. The μ_y coefficient was similar to that obtained for configuration

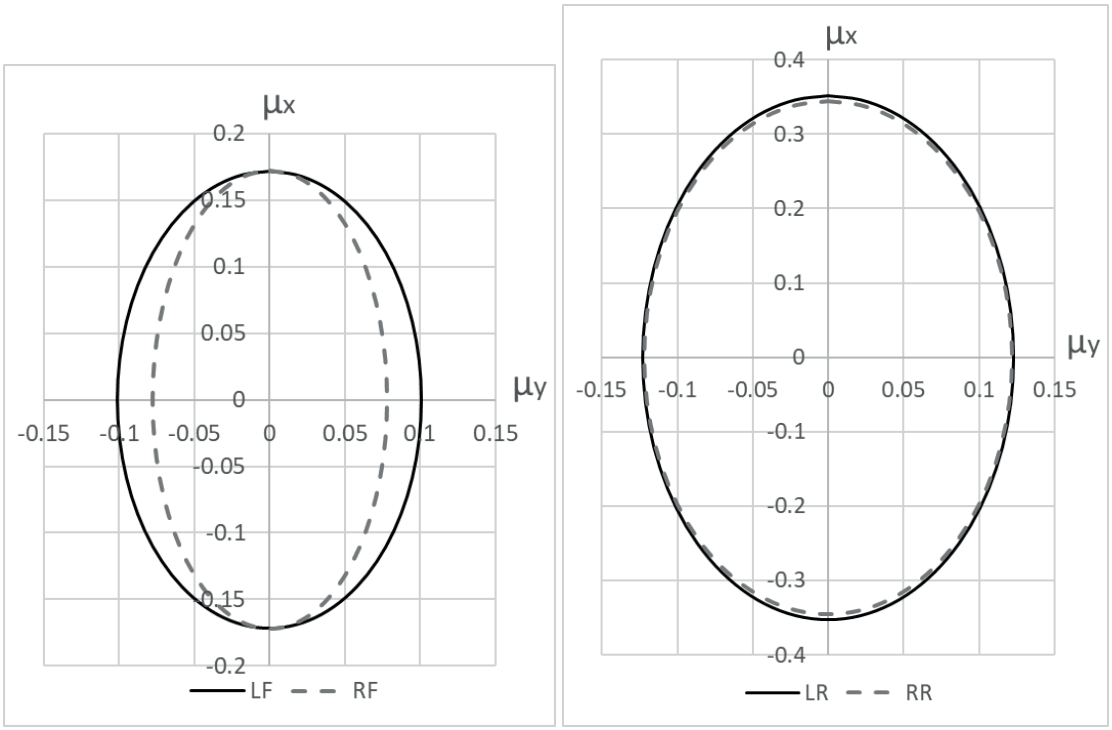

Figure 10 *Ellipses of adhesion between the wheels and the road for configuration 6*

Table 9 *The forces between the road and the wheels for configuration 7 [21]*

	Left front wheel (LF)			Right front wheel (RF)		
	F_{Xmax} [N]	F_{Ymax} [N]	F_{Zmax} [N]	F_{Xmax} [N]	F_{Ymax} [N]	F_{Zmax} [N]
Max absolute	1708.59	848.5	7734.13	2062.91	862.01	7878.1
	Left rear wheel (LR)			Right rear wheel (RR)		
	F_{Xmax} [N]	F_{Ymax} [N]	F_{Zmax} [N]	F_{Xmax} [N]	F_{Ymax} [N]	F_{Zmax} [N]
Max absolute	8049.54	1408.92	10251.4	9764.48	1149.82	10013.7

Table 10 *The forces between the road and the wheels for configuration 8 [21]*

	Left front wheel (LF)			Right front wheel (RF)		
	F_{Xmax} [N]	F_{Ymax} [N]	F_{Zmax} [N]	F_{Xmax} [N]	F_{Ymax} [N]	F_{Zmax} [N]
Max absolute	1629.48	717.01	7679.95	1822.09	722.8	7863.34
	Left rear wheel (LR)			Right rear wheel (RR)		
	F_{Xmax} [N]	F_{Ymax} [N]	F_{Zmax} [N]	F_{Xmax} [N]	F_{Ymax} [N]	F_{Zmax} [N]
Max absolute	3678.81	1111.65	10318.8	3525.51	1062.44	11779.8

5 (about 0.14 for the left and about 0.11 for the right wheel).

As for configuration 8 (the icy road included with the same intensity of the irregularities), the μ_x coefficient in the ellipse of adhesion (Figure 12) was about 0.21 for the left front and 0.23 for the right front wheel, which is greater than in the case of configuration 6 (lower amplitudes of the road irregularities). The μ_y coefficient was about 0.09, which is also similar to the results for configuration 6.

As for the rear wheels, the maximum μ_x coefficient was about 0.35 for the left and 0.3 for the right wheel, which is not entirely similar to configuration 6. The μ_y coefficient for the rear wheels was close to 0.11 for the left and about 0.09 for the right one. This was less than in the case of configuration 6.

4 Conclusions

From the presented results it can be concluded that the adopted road conditions, used in all the simulations, did not affect the lateral phenomena between the wheels and the road to any significant extent. However, when it comes to analyzing their influence on the longitudinal coefficient of adhesion the differences are

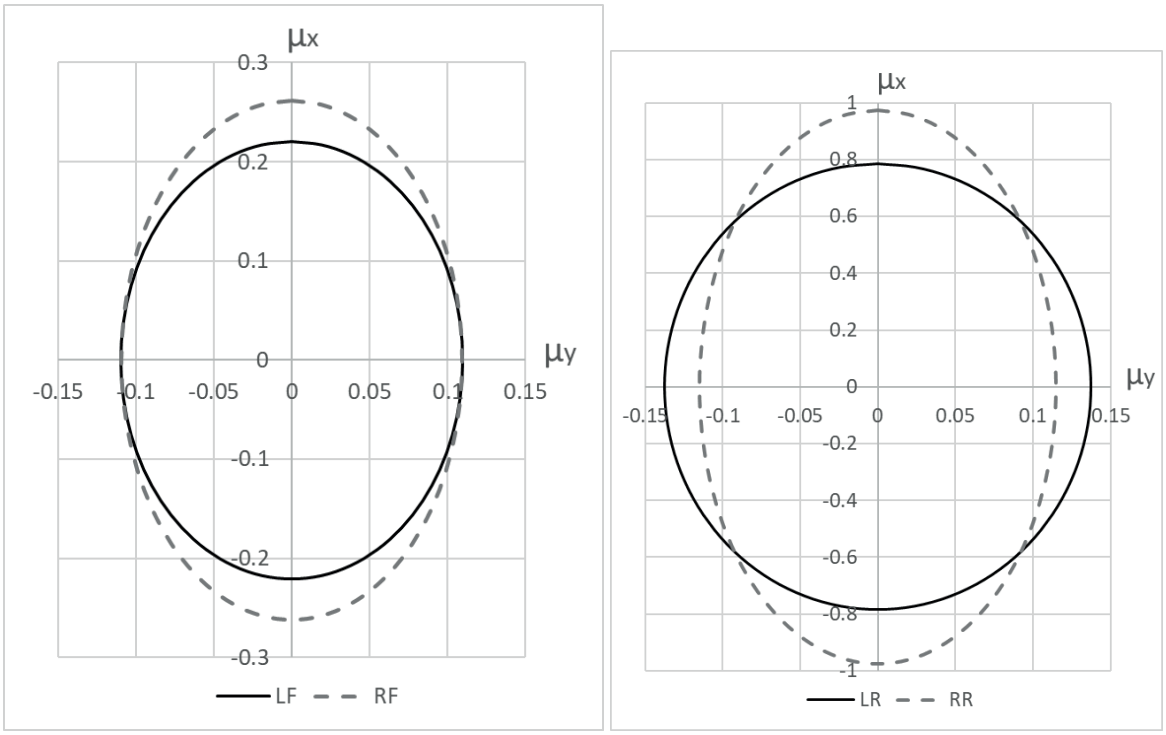

Figure 11 *Ellipses of adhesion between the wheels and the road for configuration 7*

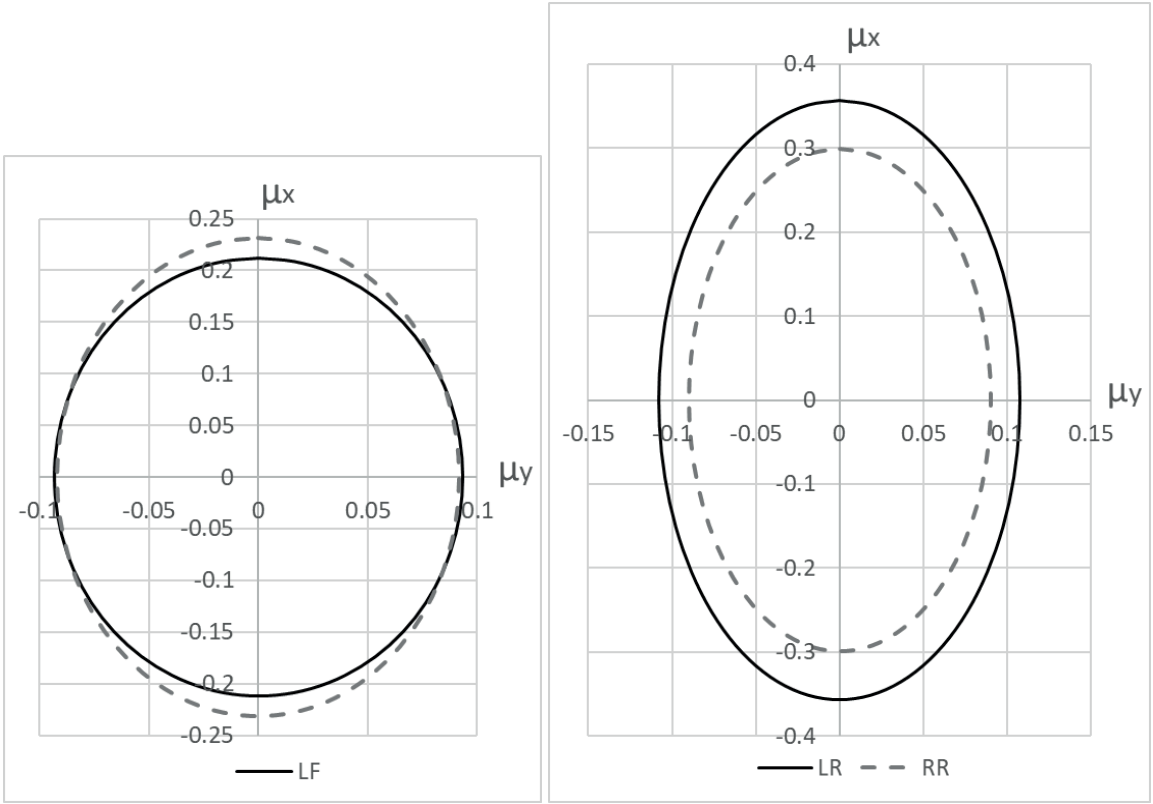

Figure 12 *Ellipses of adhesion between the wheels and the road for configuration 8*

visible, especially for the rear wheels.

The low values of the coefficient of adhesion for the front wheels of a vehicle, despite the braking maneuver, indicate that the front of a vehicle was too light and laden too poorly, versus the rear where the engine is located to generate the greater adhesion.

The rear wheels however, tended to lose their adhesion for the more harsh road conditions, especially when the icy road was included. On the dry road the highest amplitudes of the irregularities provided the increase in the maximum coefficient of longitudinal adhesion (μ_x), which seems weird when one thinks of

the potential tendency to lose contact between the road and the wheels. However, maybe the higher amplitudes caused the increase of adhesion, when the contact between the road and the wheels was regained, and the normal force increased rapidly.

The higher amplitude of the random irregularities (up to 0.022m for the intensity 0.5, up to 0.035m for the intensity 1 and up to 0.055m for the intensity 1.5) along with the icy road caused the maximum values of the coefficient of adhesion decrease significantly, especially for the rear wheels of the vehicle. This was also caused by the uneven spread of mass in the vehicle's model.

One of the important indicators in such analyses seems to be the cor_{rl} coefficient, providing almost similar or almost different road profiles.

Further research will include some other maneuvers and other loading of a vehicle, along with different values of the intensity parameter.

Acknowledgements

The authors received no financial support for the research, authorship and/or publication of this article.

Conflicts of interest

The authors declare that they have no known competing financial interests or personal relationships that could have appeared to influence the work reported in this paper.

References

[1] SHAHDEHI, I. A., ALIMARDANI, M., RAZZAGHI-KASHANI, M., ROSHANAEI, H. Adhesion and hysteretic friction of tire tread rubbers having process oils with different aromatic content. *Rubber Chemistry and Technology* [online]. 2022, **95** (4), p. 656-670. ISSN 0035-9475. Available from: https://doi.org/10.5254/rct.22.77937

[2] TOLPEKINA, T. V., PERSSON, B. N. J. Adhesion and friction for three tire tread compounds. *Lubricants* [online]. 2019, **7**(3), 20. ISSN 2075-4442. Available from: https://doi.org/10.3390/lubricants7030020

[3] ZHENG, B., HUANG, X., ZHANG, W., ZHAO, R., ZHU, S. Adhesion characteristics of tire-asphalt pavement interface based on a proposed tire hydroplaning model. *Advances in Materials Science and Engineering* [online]. 2018, **2018**, 5916180. ISSN 1687-8442. Available from: https://doi.org/10.1155/2018/5916180

[4] ZHENG, B., TANG, J., CHEN, J., ZHAO, R., HUANG, X. Investigation of adhesion properties of tire-asphalt pavement interface considering hydrodynamic lubrication action of water film on road surface. *Materials* [online]. 2022, **15**(12), 4173. ISSN 1996-1944. Available from: https://doi.org/10.3390/ma15124173

[5] ZHANG, Y., GAO, J., LI, Q. Experimental study on friction coefficients between tire tread rubber and ice. *AIP Advances* [online]. 2018, **8**(7), 075005. ISSN 2158-3226. Available from: https://doi.org/10.1063/1.5041049

[6] CABRERA, J. A., CASTILLO, J. J., PEREZ, J., VELASCO, J. M., GUERRA, A. J., HERNANDEZ, P. A. Procedure for determining tire-road friction characteristics using a modification of the magic formula based on experimental results. *Sensors* [online]. 2018, **18**(3), 896, p. 1-17. ISSN 1424-8220. Available from: https://doi.org/10.3390/s18030896

[7] MA, T., TANG, J., ZHENG, B., HUANG, X. Adhesion characteristics of vehicle tire and asphalt pavement under rainy conditions. *Journal of Beijing University of Technology* [online]. 2022, **48**(6), p. 635-643. ISSN 0254-0037. Available from: https://doi.org/10.11936/bjutxb2021090024

[8] OH, Y., LEE, H. Characteristics of a tire friction and performances of a braking in a high speed driving. *Advances in Mechanical Engineering* [online]. 2014, **6**. ISSN 1687-8140. Available from: https://doi.org/10.1155/2014/260428

[9] KHALEGHIAN, S., EMAMI, A. TAHERI, S. A technical survey on tire-road friction estimation. *Friction* [online]. 2017, **5**, p. 123-146. ISSN 2223-7690. Available from: https://doi.org/10.1007/s40544-017-0151-0

[10] ZHAO, L., ZHAO, H., CAI, J. Tire-pavement friction modeling considering pavement texture and water film, *International Journal of Transportation Science and Technology* [online]. 2023, in press. ISSN 2046-0430. Available from: https://doi.org/10.1016/j.ijtst.2023.04.001

[11] SHAOYI, B., BO, L., YANYAN, Z. Adhesion state estimation based on improved tire brush model. *Advances in Mechanical Engineering* [online]. 2018, **10**(1). ISSN 1687-8132. Available from: https://doi.org/10.1177/1687814017747706

[12] WANG, Y., HU, J., WANG, F., DONG, H., YAN, Y., REN, Y., ZHOU, CH., YIN, G. Tire road friction coefficient estimation: review and research perspectives. *Chinese Journal of Mechanical Engineering* [online]. 2022, **35**, 6. ISSN 2192-8258. Available from: https://doi.org/10.1186/s10033-021-00675-z

[13] WU, J., WANG, Y., SU, B., LIU, Q. Experimental and numerical studies on tire tread block friction characteristics based on a new test device. *Advances in Materials Science and Engineering* [online]. 2014, **2014**, 816204. ISSN 1687-8434. Available from: http://dx.doi.org/10.1155/2014/816204

[14] LENG, B., JIN, D., XIONG, L., YANG, X., YU, Z. Estimation of tire-road peak adhesion coefficient for intelligent electric vehicles based on camera and tire dynamics information fusion. *Mechanical Systems and Signal Processing* [online]. 2021, **150**, 107275. ISSN 0888-3270. Available from: https://doi.org/10.1016/j.ymssp.2020.107275

[15] HAIGERMOSER, A., LUBER, B., RAUH, J., GRAFE, G. Road and track irregularities: measurement, assessment and simulation. *Vehicle System Dynamics* [online]. 2015, **53**(7), p. 878-957. ISSN 1744-5159. Available from: https://doi.org/10.1080/00423114.2015.1037312

[16] KORTIS, J., DANIEL, L., DURATNY, M., The simulation of the influence of surface irregularities in road pavements on the response of the bridge to moving vehicle. *Procedia Engineering* [online]. 2017, **199**, p. 2991-2996. ISSN 1877-7058. Available from: https://doi.org/10.1016/j.proeng.2017.09.545

[17] NGUYEN, T., LECHNER, B., WONG, Y.D. Response-based methods to measure road surface irregularity: a state-of-the-art review. *European Transport Research Review* [online]. 2019, **11**, 43. ISSN 1866-8887. Available from: https://doi.org/10.1186/s12544-019-0380-6

[18] PRAZNOWSKI, K., MAMALA, J., SMIEJA, M., KUPINA, M. Assessment of the road surface condition with longitudinal acceleration signal of the car body. *Sensors* [online]. 2020, **20**(21), 5987. ISSN 1424-8220. Available from: https://doi.org/10.3390/s20215987

[19] RAPINO, L., LA PAGLIA, I., RIPAMONTI, F., CORRADI, R., DI LIONE, R., BARO, S. Measurement and processing of road irregularity for surface generation and tyre dynamics simulation in NVH context. *International Journal of Pavement Research and Technology* [online]. 2023. ISSN 1997-1400. Available from: https://doi.org/10.1007/s42947-023-00277-z

[20] ZHANG, J., YANG, S., LI, S., LU, Y., DING, H. Influence of vehicle-road coupled vibration on tire adhesion based on nonlinear foundation. *Applied Mathematics and Mechanics* [online]. 2021, **42**, p. 607-624. ISSN 1573-2754. Available from: https://doi.org/10.1007/s10483-021-2724-6

[21] ZALEWSKI, J. The Impact of Road Irregularities on the Motion of a Motor Vehicle during Acceleration. *Communications - Scientific Letters of the University of Zilina* [online]. 2022, **24**(2), p: 135-147. ISSN 1335-4205. Available from: doi: 10.26552/com.C.2022.2.B135-B147

[22] Adams/Tire User's Guide, MSC Software.